Observer-Based Output Feedback Integral Control for Coal-Fired Power Plant: A Three-Time-Scale Perspective

Ravindra Munje, *Member, IEEE*, Shuyi Lin, Guoqing Zhang, and Weidong Zhang, *Member, IEEE*

***Abstract*— The multivariable coal-fired power plants (CFPPs) are characterized by several interconnected nonlinear subsystems of varying time lags making the whole system stiff, and thereby attaining multitime-scale property. In this case, controls based on singular perturbation and time-scale theories provide superior results than conventional one. This brief aims to develop an integral state feedback controller with an observer using three-time-scale approach for CFPP. The integral action assures zero steady-state error, an observer determines states, and a three-time-scale technique provides flexibility to design independent subsystem controls. First, a state space model is obtained with state feedback integral action in three-time-scale form. Second, three-stage feedback control is proposed by an innovative two-time-scale separation so as to reduce design complexity and computations. Finally, an observer is constructed again by time-scale decoupling. It is then examined on the practical model of 300-MW CFPP for investigating plant behavior under various transients. In comparison, the performance of the suggested controller is found to be superior to a recently published controller.**

***Index Terms*— Integral control, power plant control, singular perturbation, three-stage design, three-time-scale system.**

I. Introduction

THE worldwide consumption of energy is expected to increase by 28% until 2040. Even if the gradual growth in renewable energy sources is estimated to be 2.3% per year from 2015 to 2040, fossil fuels remain a leader in providing 77% of the world's energy consumption in 2040 [1]. It is also predicted that the coal-fired power generation in China, which is currently about 70.31% of the total generation in China [2], is to remain somewhat constant until 2040 and the rise in the energy consumption will be compensated by renewable energy sources. However, the challenges in the operation and the control of conventional coal-fired power plants (CFPPs) are going to intensify due to the uncertainty and fluctuation of renewable energy sources when integrated into the grid. Hence, an efficient and reliable control strategy is required for CFPP.

A variety of models and controls have been studied and recommended [3], [4] over the period of time, like ARX model-based generalized predictive control [5], coordinated control [6], [7]. More recently, a nonlinear control utilizing feedback linearization along with dead-time compensation is reported in [8] for the CFPP to achieve steady closed-loop and effectual tracking performance. The same methodology is further applied to an extended model involving dynamics of superheated steam temperature [9]. Although the results obtained in [8] and [9] are superb, the studied models and controller designs are not easily configurable in conventional CFPP. In another study, a simple model based on the direct energy balance (DEB) is developed in [10], and gain scheduling PI control is employed to accomplish the tracking requirements. However, this controller is found to be poor in handling frequent variations in coal quality. Therefore, the active disturbance rejection control is devised [11]. Conversely, it counteracts the disturbance and uncertainty relatively slowly. Earlier to this, in [12], an optimal control algorithm is described for a boiler-turbine model to handle uncertainty successfully. Nevertheless, it is a state feedback-based technique which requires an observer. For that reason, an observer-based optimal linear quadratic regulator (LQR) is formulated in [13] and examined on the model presented in [12]. Similarly, H_∞-LQR [14] is also powerfully tested on a large boiler-turbine unit for enhancing demand power variation in a wide-range operation.

Coal-fired power plants (CFPPs) often exhibit a multitime-scale property due to high dimensionality and model stiffness. The direct design of feedback controls [12]–[14] for such an ill-conditioned system of the power plant, however, results in larger values of gain, making it problematic for real-time realization. This problem can be tackled by singular perturbation and time-scale methods [15]. Application of time-scale theory to power plant can be found in [16]–[18]. In [16], the time-scale structure of plant is explored and no controller is designed, whereas, in [17], the two-time-scale approach is used to design a periodic output feedback controller. In [18], a two-time-scale quasi-steady-state method is investigated for the nineth order power plant. Although the quasi-steady-state method relies on approximation, the purpose of placing subsystem eigenvalues at the exact locations is not

Manuscript received August 6, 2018; accepted October 15, 2018. Manuscript received in final form October 28, 2018. This work was supported in part by the National Science Foundation of China under Grant 61750110524, Grant 61473183, Grant 61627810, and Grant U1509211, in part by the National Key Research and Development Program of China under Grant SQ2017YFGH001005, in part by the National Postdoctoral Program for Innovative Talents under Grant BX201600103, and in part by China Postdoctoral Science Foundation under Grant 2016M601600. Recommended by Associate Editor M. Ariola. *(Corresponding author: Weidong Zhang.)*

R. Munje is with the Department of Automation, Shanghai Jiao Tong University, Shanghai 200240, China, and also with the K. K. Wagh Institute of Engineering Education and Research, Nashik 422003, India (e-mail: ravimunje@yahoo.co.in).

S. Lin is with the Department of Automation, Shanghai Jiao Tong University, Shanghai 200240, China, and also with the School of Industrial Engineering, Purdue University, West Lafayette, IN 47906, USA (e-mail: llinshuyi@sjtu.edu.cn).

G. Zhang is with the Department of Automation, Shanghai Jiao Tong University, Shanghai 200240, China, and also with the Navigation College, Dalian Maritime University, Dalian 116026, China (e-mail: zgq_dlmu@163.com).

W. Zhang is with the Department of Automation, Shanghai Jiao Tong University, Shanghai 200240, China (e-mail: wdzhang@sjtu.edu.cn).

Color versions of one or more of the figures in this brief paper are available online at http://ieeexplore.ieee.org.

Digital Object Identifier 10.1109/TCST.2018.2879045

fully satisfied. Thereof, two-stage designs [19]–[21] can be incorporated. In fact, compared to the two-time-scale method, the three-time-scale approach provides more flexibility in control design. The block-diagonalization of the three-time-scale system into "slow," "fast," and "very fast" modes is presented in [22] and [23]. Nonetheless, in both [22] and [23], control design aspects are not discussed. Recently, three-stage feedback control design for a three-time-scale system is suggested in [24] with reduced computation.

In this brief, an integral control for a three-time-scale system is proposed and investigated for the CFPP with an observer. As the control goals in traditional CFPP are excelling set-point tracking and disturbance rejection, a state feedback using integral action is recommended for a three-time-scale system. This feedback control is elicited by a more simplified three-stage design, compared to [24], averting system ill-conditioning. Furthermore, an inequality relating the proposed method and method of [24] is derived which, when satisfied, results in considerable time-saving in online computation. This controller is then applied to the practical 300-MW CFPP in which states are estimated by an observer, which is also formulated using three-stage design. The overall structure of this brief is as follows. In Section II, the model and control problem of CFPP are discussed briefly. Controller design methodology is proposed in Section III. Application of the controller to the CFPP is demonstrated in Section IV followed by the conclusion in Section V.

II. CFPP Modeling and Control Problem

A. Mathematical Modeling

A nonlinear dynamic model of 300-MW CFPP in Guangdong Province, China, is presented in [10] for DEB control. The complete model is described by

$$\frac{dq_f}{dt} = \frac{1}{c_0}\left[u_B(t-\tau) - q_f\right] \tag{1}$$

$$\frac{dD_b}{dt} = \frac{1}{c_5}\left[2.46k_c q_f^{1.230} - D_b\right] \tag{2}$$

$$\frac{dp_b}{dt} = \frac{1}{c_6}\left[D_b - 42.51 p_b^{0.956}\sqrt{p_b - p_T}\right] \tag{3}$$

$$\frac{dp_T}{dt} = \frac{1}{c_7}\left[42.51 p_b^{0.956}\sqrt{p_b - p_T} - D_T\right] \tag{4}$$

$$\frac{dp_1}{dt} = \frac{1}{c_1}[0.0083\mu_T p_T - p_1] \tag{5}$$

$$\frac{dD_T}{dt} = \frac{1}{c_2}[74.74p_1 - D_T] \tag{6}$$

with output equations

$$N_e = 0.86D_T^{0.852} \tag{7}$$

$$Q_m = p_1 + \frac{C_b}{c_6}\left[D_b - 42.51 p_b^{0.956}\sqrt{p_b - p_T}\right] \tag{8}$$

where c_0, c_1, c_2, c_5, c_6, and c_7 are inertia constants, τ is the time delay, k_c is a normalized coefficient denoting the influence of coal quality, and C_b is the thermal storage coefficient. State variables q_f, D_b, p_b, p_T, p_1, and D_T represent, respectively, mass flow rate of the coal entering into the furnace (t/h), steam production rate (t/h), drum pressure (MPa), live steam pressure (MPa), pressure in governing stage (MPa), and inlet steam mass flow rate (t/h). The outputs are electrical power (MW) and heat provided by the boiler (MPa), designated, respectively, by N_e and Q_m, while the control input u_B is the boiler demand (t/h) and μ_T is the throttle opening position (%) with the following actuator limit constraints:

$$0 \le u_B \le 150 \text{ and } 0 \le \frac{du_B}{dt} \le 0.1$$

$$0 \le \mu_T \le 100 \text{ and } 0 \le \frac{d\mu_T}{dt} \le 0.1.$$

The system (1)–(8) is linearized around steady state with $N_e = 285.9$ MW, $Q_m = 12.19$ MPa, $u_B = 122.6$ t/h, and $\mu_T = 93.5\%$. The inertia constants, τ and C_b are given in [10] and k_c is taken as 100% under steady state [11]. The linear equations, so obtained, are expressed into standard state space form as

$$\dot{\mathbf{z}} = \mathbf{A}\mathbf{z} + \mathbf{B}\mathbf{u} \tag{9}$$

$$\mathbf{y} = \mathbf{C}\mathbf{z} \tag{10}$$

where vectors $\mathbf{z}$, $\mathbf{u}$, and $\mathbf{y}$ are, respectively,

$$\mathbf{z} = \begin{bmatrix} q_f & D_b & p_b & p_T & p_1 & D_T \end{bmatrix}^T \tag{11}$$

$$\mathbf{u} = \begin{bmatrix} u_B(t-\tau) & \mu_T \end{bmatrix}^T, \mathbf{y} = \begin{bmatrix} N_e & Q_m \end{bmatrix}^T. \tag{12}$$

Note that the time delay τ in the input u_B is simulated as transport delay $e^{-\tau s}$, as done in [10]. It is seen that the system (9) is open-loop stable, i.e., $\lambda(\mathbf{A}) < 0$, where $\lambda(.)$ implies the eigenvalues of matrix. These eigenvalues are grouped into three clusters, two "slow" eigenvalues $(-0.0026, -0.0071)$, one "fast" eigenvalue (-0.0454), and three "very fast" eigenvalues $(-0.1306 \pm j0.0361, -0.2497)$. The ratios of the "slow" versus "fast" versus "very fast" modes are $\epsilon = 0.1564$ and $\mu = 0.0524$, respectively. Also, it is verified that the system is controllable, observable, and is not having zero at the origin.

B. Control Problem Description and Solution

The control of multi-input multi-output CFPP is challenging owing to the nonlinear system dynamics and the simultaneous presence of states with varying response speeds. The nonlinearity is due to the interconnections of coal-steam, steam pressure, and pressure power modules in the power plant. On the other hand, the existence of strong couplings of states with inertia lags and time constants makes the system numerically ill-conditioned. This is the reason that the control complexities are increased in narrow and wide-range operations. Thus, a well-designed controller is necessary to guarantee precise control of the entire plant, so that high efficiency and safety can be reached.

The main control objectives are: 1) the power tracking rate should be 1.5–2% of the full load per minute and reverse change of throttle pressure should be within ± 0.4 MPa [10]; 2) regardless of the transients in the power plant input variables; output and state variables should be quickly regulated; and 3) the plant output variables should be insensitive to the coal quality and large parameter variations.

The aforementioned control requirements are met by proposing a control configuration as: 1) the system state space representation is obtained for integral state feedback control to achieve the output tracking performance and insensitivity to disturbances and parameter variations; 2) the stabilizing

feedback gain, for the above-mentioned three-time-scale system, is determined by three-stage design to get rid of the ill-conditioning of the system matrix; and 3) the limitation of the state feedback is overcome by employing an observer, obtained by the similar three-stage design.

III. Proposed Control Design

In this section, state feedback with integral control is designed and realized via an observer for a three-time-scale system. At first, integral state feedback control using an observer is discussed in short. Subsequently, its application to a three-time-scale system is proposed.

A. Observer-Based Output Feedback Integral Control

Consider a linear time-invariant continuous-time system as

$$\dot{\mathbf{z}} = \mathbf{A}\mathbf{z} + \mathbf{B}\mathbf{u} \tag{13}$$

$$\mathbf{y} = \mathbf{C}\mathbf{z} \tag{14}$$

where $\mathbf{z} \in \Re^n$, $\mathbf{u} \in \Re^m$, and $\mathbf{y} \in \Re^p$. The matrices $\mathbf{A}$, $\mathbf{B}$, and $\mathbf{C}$ are of suitable dimensions.

Assumption 1: $(\mathbf{A}, \mathbf{B}, \mathbf{C})$ is controllable and observable.

Assumption 2: The system $\mathbf{G}(s) = \mathbf{C}[s\mathbf{I}_n - \mathbf{A}]^{-1}\mathbf{B}$ does not have transmission zeros at the origin [25].

Assumption 1 is necessary for the design of feedback and observer gains, whereas Assumption 2 is the requirement of tracking control promoting integral action. If the parameters of the system (13)-(14) are not known exactly, an asymptotic tracking may not be attained. In this case, an integral control could be used to achieve it. Also, the closed-loop system with integral action becomes more robust as long as the designed system is stable. For the same, let us augment the system (13)-(14) with

$$\dot{\mathbf{z}}_y = \mathbf{y} - \mathbf{y}_{\text{ref}} \tag{15}$$

where $\mathbf{y}_{\text{ref}} \in \Re^p$ is the reference output vector. Thus, from (13)–(15), the overall system is assembled as

$$\dot{\mathbf{x}} = \hat{\mathbf{A}}\mathbf{x} + \hat{\mathbf{B}}\mathbf{u} + \hat{\mathbf{E}}\mathbf{y}_{\text{ref}} \tag{16}$$

$$\mathbf{y} = \hat{\mathbf{C}}\mathbf{x} \tag{17}$$

where $\mathbf{x} = [\mathbf{z}_y^T \mathbf{z}^T]^T$ and

$$\hat{\mathbf{A}} = \begin{bmatrix} \mathbf{0} & \mathbf{C} \\ \mathbf{0} & \mathbf{A} \end{bmatrix}, \quad \hat{\mathbf{B}} = \begin{bmatrix} \mathbf{0} \\ \mathbf{B} \end{bmatrix}, \quad \hat{\mathbf{E}} = \begin{bmatrix} -\mathbf{I}_p \\ \mathbf{0} \end{bmatrix}, \quad \hat{\mathbf{C}} = \begin{bmatrix} \mathbf{0} \\ \mathbf{C}^T \end{bmatrix}^T$$

in which $\mathbf{I}_p$ is an identity matrix of order p and $\mathbf{0}$ is null matrix of proper order. The controllability of (16) is guaranteed, if the Assumptions 1 and 2 are satisfied [25]. Thus, all the eigenvalues of (16) can be placed arbitrarily by selecting feedback gain $\hat{\mathbf{K}}$. As a result, the control input

$$\mathbf{u} = -\hat{\mathbf{K}}\mathbf{x} = -\begin{bmatrix} \mathbf{K}_y & \mathbf{K} \end{bmatrix}\begin{bmatrix} \mathbf{z}_y^T & \mathbf{z}^T \end{bmatrix}^T \tag{18}$$

is applied to the system (16). Then

$$\dot{\mathbf{x}} = \mathbf{A}_{cl}\mathbf{x} + \hat{\mathbf{E}}\mathbf{y}_{\text{ref}} \tag{19}$$

$$\mathbf{y} = \hat{\mathbf{C}}\mathbf{x} \tag{20}$$

where $\mathbf{A}_{cl} = \hat{\mathbf{A}} - \hat{\mathbf{B}}\hat{\mathbf{K}}$. An asymptotic set-point tracking can also be interpreted by the transfer function of (19)-(20) as

$$\mathbf{G}_{cl}(s) = \hat{\mathbf{C}}[s\mathbf{I}_{n+p} - \mathbf{A}_{cl}]^{-1}\hat{\mathbf{E}}. \tag{21}$$

Here, the dc-gain of (21) is 1, implying reference tracking. However, most of the times system states are unavailable for feedback. In that case, using Assumption 1, state observer can be built. Therefore, the control (18) is replaced with

$$\mathbf{u} = -\mathbf{K}_y\mathbf{z}_y - \mathbf{K}\hat{\mathbf{z}} \tag{22}$$

where $\hat{\mathbf{z}}$ is an estimated state vector with $\mathbf{e} = \mathbf{z} - \hat{\mathbf{z}}$ satisfying

$$\dot{\mathbf{e}} = (\mathbf{A} - \mathbf{L}\mathbf{C})\mathbf{e} \tag{23}$$

with $\mathbf{L}$ as an observer gain for (13)-(14). Then, control (22)

$$\mathbf{u} = -\mathbf{K}_y\mathbf{z}_y - \mathbf{K}\mathbf{z} + \mathbf{K}\mathbf{e}. \tag{24}$$

Substituting (24) into (16) and combining with (23) yield

$$\dot{\zeta} = \mathbf{A}_{\text{aug}}\zeta + \mathbf{B}_{\text{aug}}\mathbf{y}_{\text{ref}} \tag{25}$$

$$\mathbf{y} = \mathbf{C}_{\text{aug}}\zeta \tag{26}$$

where $\zeta = [\mathbf{z}_y^T \mathbf{z}^T \mathbf{e}^T]^T$ and

$$\mathbf{A}_{\text{aug}} = \left[\begin{array}{ccc} \mathbf{0} & \mathbf{C} & \mathbf{0} \\ -\mathbf{B}\mathbf{K}_y & \mathbf{A} - \mathbf{B}\mathbf{K} & \mathbf{B}\mathbf{K} \\ \hline \mathbf{0} & \mathbf{0} & \mathbf{A} - \mathbf{L}\mathbf{C} \end{array}\right] = \begin{bmatrix} \hat{\mathbf{A}} - \hat{\mathbf{B}}\hat{\mathbf{K}} & \hat{\mathbf{B}}\mathbf{K} \\ \mathbf{0} & \mathbf{A} - \mathbf{L}\mathbf{C} \end{bmatrix}$$

$$\mathbf{B}_{\text{aug}} = \begin{bmatrix} -\mathbf{I}_p \\ \mathbf{0} \\ \hline \mathbf{0} \end{bmatrix} = \begin{bmatrix} \hat{\mathbf{E}} \\ \mathbf{0} \end{bmatrix}, \mathbf{C}_{\text{aug}} = \left[\begin{array}{c} \mathbf{0} \\ \mathbf{C}^T \\ \hline \mathbf{0} \end{array}\right]^T = \begin{bmatrix} \hat{\mathbf{C}}^T \\ \mathbf{0} \end{bmatrix}^T.$$

It is important to note that

$$\mathbf{G}_{cl}(s) = \mathbf{C}_{\text{aug}}[s\mathbf{I}_{2n+p} - \mathbf{A}_{\text{aug}}]^{-1}\mathbf{B}_{\text{aug}} \tag{27}$$

is similar to (21). Thus, the reference tracking properties of the system are conserved in the presence of plant parameter variations and disturbances whether the integral state feedback or observer-based integral output feedback is employed.

B. Controller Synthesis for Three-Time-Scale System

Three-time-scale systems are characterized by the three widely separated groups of eigenvalues emerging into an overall stiff system, demanding expensive algebraic routines for feedback and observer gain designs. Perversely computational complexity arising due to three-time-scale nature can be efficiently handled by advised three-stage design for both feedback gain $\hat{\mathbf{K}}$ for (16)-(17) and observer gain $\mathbf{L}$ for (13)-(14). Before proceeding, following Lemma 1 is introduced.

Lemma 1: If the system (13)-(14) exhibits three-time-scale property, with n_1 "slow," n_2 "fast," and n_3 "very fast" modes, such that $n_1 + n_2 + n_3 = n$, then the system (16)-(17) of order $n + p$ also bears three-time-scale form with "slow," "fast," and "very fast" modes, respectively, of orders $n_1 + p$, n_2, and n_3.

Proof: The eigenvalues of the systems (13)-(14) and (16)-(17) can, respectively, be given by the characteristic equations

$$D_1(s) = \det\left[s\mathbf{I}_n - \mathbf{A}\right] \tag{28}$$

$$D_2(s) = \det\begin{bmatrix} s\mathbf{I}_p & -\mathbf{C} \\ \mathbf{0} & s\mathbf{I}_n - \mathbf{A} \end{bmatrix}. \tag{29}$$

It is apparent that, the solution of (29) adds p eigenvalues at the origin to the solution of (28) which already has

n_1 "slow," n_2 "fast," and n_3 "very fast" eigenvalue modes. The modes of the system are decided by absolute eigenvalues, i.e., eigenvalues near to the imaginary axis are clubbed as "slow," far and farther from the imaginary axis as "fast" and "very fast," respectively. Consequently, p eigenvalues at origin are undoubtedly counted in "slow" mode, which increases the order of slow mode of the system (16)-(17) from n_1 to n_1+p without changing the eigenvalues in the "fast" and "very fast" modes. ■

Mostly, "fast" and "very fast" modes are stable but "slow" ones are unstable. And, when integral state feedback control is attempted then again "p" poles are added at the origin, which further boosts instability. For such systems, the straightforward design of (18) is computationally tough. This is equally true for observer gain in (23). Hence, these gains are designed in three stages using the two-time-scale method, by regrouping of states. As the design is based on similarity transformations, Assumption 1 is also applicable to decoupled subsystems. Here, the design procedure for $\hat{\mathbf{K}}$ is conveyed first and then for $\mathbf{L}$.

1) Design of Feedback Gain ($\hat{\mathbf{K}}$)*:* Let (13)-(14) be represented into standard singularly perturbed three-time-scale form

$$\begin{bmatrix}\dot{\mathbf{z}}_1\\ \dot{\mathbf{z}}_2\\ \dot{\mathbf{z}}_3\end{bmatrix}=\begin{bmatrix}\mathbf{A}_{o11} & \mathbf{A}_{o12} & \mathbf{A}_{o13}\\ \frac{\mathbf{A}_{o21}}{\epsilon} & \frac{\mathbf{A}_{o22}}{\epsilon} & \frac{\mathbf{A}_{o23}}{\epsilon}\\ \frac{\mathbf{A}_{o31}}{\mu} & \frac{\mathbf{A}_{o32}}{\mu} & \frac{\mathbf{A}_{o33}}{\mu}\end{bmatrix}\begin{bmatrix}\mathbf{z}_1\\ \mathbf{z}_2\\ \mathbf{z}_3\end{bmatrix}+\begin{bmatrix}\mathbf{B}_{o1}\\ \frac{\mathbf{B}_{o2}}{\epsilon}\\ \frac{\mathbf{B}_{o3}}{\mu}\end{bmatrix}\mathbf{u} \quad (30)$$

$$\mathbf{y}=\begin{bmatrix}\mathbf{C}_{o1} & \mathbf{C}_{o2} & \mathbf{C}_{o3}\end{bmatrix}\begin{bmatrix}\mathbf{z}_1^T & \mathbf{z}_2^T & \mathbf{z}_3^T\end{bmatrix}^T \quad (31)$$

where $\mathbf{z}_1\in\Re^{n_1}$, $\mathbf{z}_2\in\Re^{n_2}$, and $\mathbf{z}_3\in\Re^{n_3}$ are, respectively, slow, fast, and very fast states, $\mathbf{u}\in\Re^m$ is input and $\mathbf{y}\in\Re^p$ is output. $\mathbf{A}_{oij}$, $\mathbf{B}_{oi}$, and $\mathbf{C}_{oi}$ are of appropriate dimensions (subscript "o" stands for original system). Parameters ϵ and μ are speed ratios of $\mathbf{z}_1$ versus $\mathbf{z}_2$ versus $\mathbf{z}_3$ states, such that $\mu\ll\epsilon\ll 1$.

Assumption 3: $\mathbf{A}_{o22}$ and $\mathbf{A}_{o33}$ are invertible [26].

This is standard assumption, needed to get solutions of algebraic equations treated in this section. Now, augmenting the system (30)-(31) with (15), following singularly perturbed form of (16)-(17), as proved in Lemma 1, is obtained

$$\begin{bmatrix}\dot{\mathbf{x}}_1\\ \dot{\mathbf{x}}_2\\ \dot{\mathbf{x}}_3\end{bmatrix}=\begin{bmatrix}\mathbf{A}_{11} & \mathbf{A}_{12} & \mathbf{A}_{13}\\ \frac{\mathbf{A}_{21}}{\epsilon} & \frac{\mathbf{A}_{22}}{\epsilon} & \frac{\mathbf{A}_{23}}{\epsilon}\\ \frac{\mathbf{A}_{31}}{\mu} & \frac{\mathbf{A}_{32}}{\mu} & \frac{\mathbf{A}_{33}}{\mu}\end{bmatrix}\begin{bmatrix}\mathbf{x}_1\\ \mathbf{x}_2\\ \mathbf{x}_3\end{bmatrix}+\begin{bmatrix}\mathbf{B}_1\\ \frac{\mathbf{B}_2}{\epsilon}\\ \frac{\mathbf{B}_3}{\mu}\end{bmatrix}\mathbf{u}+\begin{bmatrix}\hat{\mathbf{E}}\\ \mathbf{0}\\ \mathbf{0}\end{bmatrix}\mathbf{y}_{\text{ref}} \quad (32)$$

$$\mathbf{y}=\begin{bmatrix}\mathbf{C}_1 & \mathbf{C}_2 & \mathbf{C}_3\end{bmatrix}\begin{bmatrix}\mathbf{x}_1^T & \mathbf{x}_2^T & \mathbf{x}_3^T\end{bmatrix}^T \quad (33)$$

where $\mathbf{x}_1=[\mathbf{z}_y^T\ \mathbf{z}_1^T]^T$, $\mathbf{x}_2=\mathbf{z}_2$, and $\mathbf{x}_3=\mathbf{z}_3$ with appropriate regrouping of matrices $\mathbf{A}_{ij}$, $\mathbf{B}_i$, and $\mathbf{C}_i$, respectively. Matrix $\hat{\mathbf{E}}=[-\mathbf{I}_p\ \mathbf{0}]^T$ with $\mathbf{0}$ as null matrix of dimension $n_1\times p$. As assumed that the matrices $\mathbf{A}_{o22}$ and $\mathbf{A}_{o33}$ are invertible, $\mathbf{A}_{22}$ and $\mathbf{A}_{33}$ are also invertible. Because, $\mathbf{A}_{22}=\mathbf{A}_{o22}$ and $\mathbf{A}_{33}=\mathbf{A}_{o33}$. Here, the main objective is to design a feedback gain $\hat{\mathbf{K}}$, so that the system (16)-(17) [i.e., (32)-(33)] is stabilized, i.e., $\lambda(\hat{\mathbf{A}}-\hat{\mathbf{B}}\hat{\mathbf{K}})<0$. As the application of input (18) to the system (16) keeps the term $\hat{\mathbf{E}}\mathbf{y}_{\text{ref}}$ in (19) unchanged, it is not considered further in designing control.

First of all, system (32) is transformed into lower triangular form, and then, three-stage design is carried out. For simplifying the design, consider state regrouping of the system (32) as

$$\mathbf{x}_a=\begin{bmatrix}\mathbf{x}_1^T & \mathbf{x}_2^T\end{bmatrix}^T \text{ and } \mathbf{x}_b=\mathbf{x}_3. \quad (34)$$

Therefore, the system (32) can be rewritten as

$$\begin{bmatrix}\dot{\mathbf{x}}_a\\ \dot{\mathbf{x}}_b\end{bmatrix}=\begin{bmatrix}\bar{\mathbf{A}}_{11} & \bar{\mathbf{A}}_{12}\\ \frac{\bar{\mathbf{A}}_{21}}{\mu} & \frac{\bar{\mathbf{A}}_{22}}{\mu}\end{bmatrix}\begin{bmatrix}\mathbf{x}_a\\ \mathbf{x}_b\end{bmatrix}+\begin{bmatrix}\bar{\mathbf{B}}_1\\ \frac{\bar{\mathbf{B}}_2}{\mu}\end{bmatrix}\mathbf{u} \quad (35)$$

where $\bar{\mathbf{A}}_{ij}$ and $\bar{\mathbf{B}}_i$ are reorganized accordingly. The system (35) is the two-time-scale representation of system (32), where n_1+p "slow" and n_2 "fast" states are merged to form (n_1+n_2+p) "slow" states and n_3 "very fast" states are taken as "fast" states. Now, the application of transformation

$$\mathbf{x}_s=\mathbf{x}_a+\mu\mathbf{P}\mathbf{x}_b \quad (36)$$

to the system (35), produces

$$\begin{bmatrix}\dot{\mathbf{x}}_s\\ \dot{\mathbf{x}}_b\end{bmatrix}=\begin{bmatrix}\bar{\mathbf{A}}_s & \mathbf{0}\\ \frac{\bar{\mathbf{A}}_{21}}{\mu} & \frac{\bar{\mathbf{A}}_f}{\mu}\end{bmatrix}\begin{bmatrix}\mathbf{x}_s\\ \mathbf{x}_b\end{bmatrix}+\begin{bmatrix}\bar{\mathbf{B}}_s\\ \frac{\bar{\mathbf{B}}_2}{\mu}\end{bmatrix}\mathbf{u} \quad (37)$$

where $\bar{\mathbf{A}}_s=\bar{\mathbf{A}}_{11}+\mathbf{P}\bar{\mathbf{A}}_{21}$, $\bar{\mathbf{A}}_f=\bar{\mathbf{A}}_{22}-\mu\bar{\mathbf{A}}_{21}\mathbf{P}$, and $\bar{\mathbf{B}}_s=\bar{\mathbf{B}}_1+\mathbf{P}\bar{\mathbf{B}}_2$. As $\mathbf{A}_{33}$, i.e., $\bar{\mathbf{A}}_{22}$ is invertible (Assumption 3), the unique solution of $\mathbf{P}$ can be obtained by solving

$$\bar{\mathbf{A}}_{12}+\mathbf{P}\bar{\mathbf{A}}_{22}-\mu(\bar{\mathbf{A}}_{11}+\mathbf{P}\bar{\mathbf{A}}_{21})\mathbf{P}=0 \quad (38)$$

iteratively for sufficiently small value of μ [26]. Consequently, the system (37) is modeled into lower triangular form, where $\mathbf{x}_s$ is completely decoupled from $\mathbf{x}_b$ and it is given by

$$\dot{\mathbf{x}}_s=\bar{\mathbf{A}}_s\mathbf{x}_s+\bar{\mathbf{B}}_s\mathbf{u}. \quad (39)$$

Recall that, $\mathbf{x}_s$ combines (n_1+p) "slow" and n_2 "fast" states of the system (32). Hence, it can also be written in two-time-scale form, by partitioning $\bar{\mathbf{A}}_s$ and $\bar{\mathbf{B}}_s$ suitably, as

$$\begin{bmatrix}\dot{\mathbf{x}}_{s1}\\ \dot{\mathbf{x}}_{s2}\end{bmatrix}=\begin{bmatrix}\bar{\mathbf{A}}_{s11} & \bar{\mathbf{A}}_{s12}\\ \frac{\bar{\mathbf{A}}_{s21}}{\epsilon} & \frac{\bar{\mathbf{A}}_{s22}}{\epsilon}\end{bmatrix}\begin{bmatrix}\mathbf{x}_{s1}\\ \mathbf{x}_{s2}\end{bmatrix}+\begin{bmatrix}\bar{\mathbf{B}}_{s1}\\ \frac{\bar{\mathbf{B}}_{s2}}{\epsilon}\end{bmatrix}\mathbf{u} \quad (40)$$

where $\mathbf{x}_s=[\mathbf{x}_{s1}^T\mathbf{x}_{s2}^T]^T$ with $\mathbf{x}_{s1}\in\Re^{n_1+p}$ and $\mathbf{x}_{s2}\in\Re^{n_2}$. At this moment, a linear transformation

$$\mathbf{x}_{ss}=\mathbf{x}_{s1}+\epsilon\mathbf{P}_s\mathbf{x}_{s2} \quad (41)$$

is applied to (40). Here, $\mathbf{P}_s$ is determined by solving

$$\bar{\mathbf{A}}_{s12}+\mathbf{P}_s\bar{\mathbf{A}}_{s22}-\epsilon(\bar{\mathbf{A}}_{s11}+\mathbf{P}_s\bar{\mathbf{A}}_{s21})\mathbf{P}_s=0. \quad (42)$$

Solution of $\mathbf{P}_s$ is obtained under Assumption 3 that $\mathbf{A}_{22}$, i.e., $\bar{\mathbf{A}}_{s22}$ is invertible for a small value of ϵ. Accordingly, a lower triangular form of (40) is obtained as

$$\begin{bmatrix}\dot{\mathbf{x}}_{ss}\\ \dot{\mathbf{x}}_{s2}\end{bmatrix}=\begin{bmatrix}\bar{\mathbf{A}}_{ss} & \mathbf{0}\\ \frac{\bar{\mathbf{A}}_{s21}}{\epsilon} & \frac{\bar{\mathbf{A}}_{sf}}{\epsilon}\end{bmatrix}\begin{bmatrix}\mathbf{x}_{ss}\\ \mathbf{x}_{s2}\end{bmatrix}+\begin{bmatrix}\bar{\mathbf{B}}_{ss}\\ \frac{\bar{\mathbf{B}}_{s2}}{\epsilon}\end{bmatrix}\mathbf{u} \quad (43)$$

where $\bar{\mathbf{A}}_{ss}=\bar{\mathbf{A}}_{s11}+\mathbf{P}_s\bar{\mathbf{A}}_{s21}$, $\bar{\mathbf{A}}_{sf}=\bar{\mathbf{A}}_{s22}-\epsilon\bar{\mathbf{A}}_{s21}\mathbf{P}_s$, and $\bar{\mathbf{B}}_{ss}=\bar{\mathbf{B}}_{s1}+\mathbf{P_s}\bar{\mathbf{B}}_{s2}$. Thus, using block triangular forms (37) and (43) of two-time-scale representations, the original three-time-scale system (32) is converted into block triangular form

$$\begin{bmatrix}\dot{\mathbf{x}}_{ss}\\ \dot{\mathbf{x}}_{s2}\\ \dot{\mathbf{x}}_3\end{bmatrix}=\begin{bmatrix}\bar{\mathbf{A}}_{ss} & \mathbf{0} & \mathbf{0}\\ \frac{\bar{\mathbf{A}}_{s21}}{\epsilon} & \frac{\bar{\mathbf{A}}_{sf}}{\epsilon} & \mathbf{0}\\ \frac{\bar{\mathbf{A}}_{31}}{\mu} & \frac{\bar{\mathbf{A}}_{32}}{\mu} & \frac{\bar{\mathbf{A}}_f}{\mu}\end{bmatrix}\begin{bmatrix}\mathbf{x}_{ss}\\ \mathbf{x}_{s2}\\ \mathbf{x}_3\end{bmatrix}+\begin{bmatrix}\bar{\mathbf{B}}_{ss}\\ \frac{\bar{\mathbf{B}}_{s2}}{\epsilon}\\ \frac{\bar{\mathbf{B}}_2}{\mu}\end{bmatrix}\mathbf{u} \quad (44)$$

where $\bar{\mathbf{A}}_{21}$ in (37) is appropriately partitioned as $[\bar{\mathbf{A}}_{31}\ \bar{\mathbf{A}}_{32}]$.

Now, one can proceed for three-stage feedback control design starting with the "slow" subsystem $\mathbf{x}_{ss}$. To begin with, the control is designed for the system (40) and then for the system (35). In the first stage, applying feedback control

$$\mathbf{u} = -\mathbf{K}_{ss}\mathbf{x}_{ss} + \mathbf{u}_{sf} \tag{45}$$

to the system (43), leads to

$$\begin{bmatrix}\dot{\mathbf{x}}_{ss}\\ \dot{\mathbf{x}}_{s2}\end{bmatrix} = \begin{bmatrix}\bar{\mathbf{A}}_{ss}-\bar{\mathbf{B}}_{ss}\mathbf{K}_{ss} & \mathbf{0}\\ \frac{\bar{\mathbf{A}}_{s21}-\bar{\mathbf{B}}_{s2}\mathbf{K}_{ss}}{\epsilon} & \frac{\bar{\mathbf{A}}_{sf}}{\epsilon}\end{bmatrix}\begin{bmatrix}\mathbf{x}_{ss}\\ \mathbf{x}_{s2}\end{bmatrix} + \begin{bmatrix}\bar{\mathbf{B}}_{ss}\\ \frac{\bar{\mathbf{B}}_{s2}}{\epsilon}\end{bmatrix}\mathbf{u}_{sf} \tag{46}$$

where $\mathbf{K}_{ss}$ is selected such that $\lambda(\bar{\mathbf{A}}_{ss}-\bar{\mathbf{B}}_{ss}\mathbf{K}_{ss})$ are "slow" and in left half of s-plane. Now, using change of the variables

$$\mathbf{x}_{sf} = -\mathbf{M}_s\mathbf{x}_{ss} + \mathbf{x}_{s2} \tag{47}$$

the system (46) is modified to block diagonal form

$$\begin{bmatrix}\dot{\mathbf{x}}_{ss}\\ \dot{\mathbf{x}}_{sf}\end{bmatrix} = \begin{bmatrix}\bar{\mathbf{A}}_{ss}-\bar{\mathbf{B}}_{ss}\mathbf{K}_{ss} & \mathbf{0}\\ \mathbf{0} & \frac{\bar{\mathbf{A}}_{sf}}{\epsilon}\end{bmatrix}\begin{bmatrix}\mathbf{x}_{ss}\\ \mathbf{x}_{sf}\end{bmatrix} + \begin{bmatrix}\bar{\mathbf{B}}_{ss}\\ \frac{\bar{\mathbf{B}}_{sf}}{\epsilon}\end{bmatrix}\mathbf{u}_{sf} \tag{48}$$

where $\bar{\mathbf{B}}_{sf} = \bar{\mathbf{B}}_{s2} - \epsilon\mathbf{M}_s\bar{\mathbf{B}}_{ss}$ and matrix $\mathbf{M}_s$ satisfies

$$\bar{\mathbf{A}}_{s21} - \bar{\mathbf{B}}_{s2}\mathbf{K}_{ss} - \epsilon\mathbf{M}_s(\bar{\mathbf{A}}_{ss}-\bar{\mathbf{B}}_{ss}\mathbf{K}_{ss}) + \bar{\mathbf{A}}_{sf}\mathbf{M}_s = 0. \tag{49}$$

Solution of (49) exists if Assumption 4 is satisfied.

Assumption 4: $\lambda(\bar{\mathbf{A}}_{ss}-\bar{\mathbf{B}}_{ss}\mathbf{K}_{ss}) \neq \lambda(\bar{\mathbf{A}}_{sf}/\epsilon)$.

It is satisfied because $(\bar{\mathbf{A}}_{ss}-\bar{\mathbf{B}}_{ss}\mathbf{K}_{ss})$ is user designed and has desired "slow" eigenvalues, while $\frac{\bar{\mathbf{A}}_{sf}}{\epsilon}$ has original "fast" subsystem eigenvalues. In (48), subsystem $\mathbf{x}_{sf}$ is made totally independent of $\mathbf{x}_{ss}$. Thus, in the second stage

$$\mathbf{u}_{sf} = -\mathbf{K}_{sf}\mathbf{x}_{sf} \tag{50}$$

is applied to the system (48) as

$$\begin{bmatrix}\dot{\mathbf{x}}_{ss}\\ \dot{\mathbf{x}}_{sf}\end{bmatrix} = \begin{bmatrix}\bar{\mathbf{A}}_{ss}-\bar{\mathbf{B}}_{ss}\mathbf{K}_{ss} & -\bar{\mathbf{B}}_{ss}\mathbf{K}_{sf}\\ \mathbf{0} & \frac{\bar{\mathbf{A}}_{sf}-\bar{\mathbf{B}}_{sf}\mathbf{K}_{sf}}{\epsilon}\end{bmatrix}\begin{bmatrix}\mathbf{x}_{ss}\\ \mathbf{x}_{sf}\end{bmatrix} \tag{51}$$

so that $\lambda((\bar{\mathbf{A}}_{sf}-\bar{\mathbf{B}}_{sf}\mathbf{K}_{sf})/\epsilon)$ are made asymptotically stable. Thus, the overall input for the system (40) is computed using transformations (41) and (47) and controls (45) and (50) as

$$\mathbf{u} = -\mathbf{K}_s\begin{bmatrix}\mathbf{x}_{s1}^T & \mathbf{x}_{s2}^T\end{bmatrix}^T = -\mathbf{K}_s\mathbf{x}_s \tag{52}$$

where

$$\mathbf{K}_s = \begin{bmatrix}\mathbf{K}_{ss}-\mathbf{K}_{sf}\mathbf{M}_s & \epsilon(\mathbf{K}_{ss}-\mathbf{K}_{sf}\mathbf{M}_s)\mathbf{P}_s + \mathbf{K}_{sf}\end{bmatrix}. \tag{53}$$

Actually, (52) is the input for (39), which is the decoupled part of (37). Therefore, the overall input (52) has the form

$$\mathbf{u} = -\mathbf{K}_s\mathbf{x}_s + \mathbf{u}_f \tag{54}$$

and is passed on to the system (37). This results in

$$\begin{bmatrix}\dot{\mathbf{x}}_s\\ \dot{\mathbf{x}}_b\end{bmatrix} = \begin{bmatrix}\bar{\mathbf{A}}_s-\bar{\mathbf{B}}_s\mathbf{K}_s & \mathbf{0}\\ \frac{\bar{\mathbf{A}}_{21}-\bar{\mathbf{B}}_2\mathbf{K}_s}{\mu} & \frac{\bar{\mathbf{A}}_f}{\mu}\end{bmatrix}\begin{bmatrix}\mathbf{x}_s\\ \mathbf{x}_b\end{bmatrix} + \begin{bmatrix}\bar{\mathbf{B}}_s\\ \frac{\bar{\mathbf{B}}_2}{\mu}\end{bmatrix}\mathbf{u}_f. \tag{55}$$

Once again introducing change of coordinates as

$$\mathbf{x}_f = -\mathbf{M}\mathbf{x}_s + \mathbf{x}_b \tag{56}$$

for the system (55), subsystem $\mathbf{x}_f$ is isolated from $\mathbf{x}_s$ as

$$\begin{bmatrix}\dot{\mathbf{x}}_s\\ \dot{\mathbf{x}}_f\end{bmatrix} = \begin{bmatrix}\bar{\mathbf{A}}_s-\bar{\mathbf{B}}_s\mathbf{K}_s & \mathbf{0}\\ \mathbf{0} & \frac{\bar{\mathbf{A}}_f}{\mu}\end{bmatrix}\begin{bmatrix}\mathbf{x}_s\\ \mathbf{x}_f\end{bmatrix} + \begin{bmatrix}\bar{\mathbf{B}}_s\\ \frac{\bar{\mathbf{B}}_f}{\mu}\end{bmatrix}\mathbf{u}_f \tag{57}$$

where $\bar{\mathbf{B}}_f = \bar{\mathbf{B}}_2 - \mu\mathbf{M}\bar{\mathbf{B}}_s$ and $\mathbf{M}$ is evaluated by setting

$$\bar{\mathbf{A}}_{21} - \bar{\mathbf{B}}_2\mathbf{K}_s - \mu\mathbf{M}(\bar{\mathbf{A}}_s - \bar{\mathbf{B}}_s\mathbf{K}_s) + \bar{\mathbf{A}}_f\mathbf{M} = 0. \tag{58}$$

Assumption 5 is needed to solve (58).

Assumption 5: $\lambda(\bar{\mathbf{A}}_s - \bar{\mathbf{B}}_s\mathbf{K}_s) \neq \lambda(\bar{\mathbf{A}}_f/\mu)$.

And, it can be convinced by the fact that $(\bar{\mathbf{A}}_s - \bar{\mathbf{B}}_s\mathbf{K}_s)$ is designed with desired eigenvalues laying in "slow" and "fast" dynamic modes and $\frac{\bar{\mathbf{A}}_f}{\mu}$ has "very fast" eigenvalues of full-order system. Finally, in the third stage

$$\mathbf{u}_f = -\mathbf{K}_f\mathbf{x}_f \tag{59}$$

is applied to the system (57) as

$$\begin{bmatrix}\dot{\mathbf{x}}_s\\ \dot{\mathbf{x}}_f\end{bmatrix} = \begin{bmatrix}\bar{\mathbf{A}}_s-\bar{\mathbf{B}}_s\mathbf{K}_s & -\bar{\mathbf{B}}_s\mathbf{K}_f\\ \mathbf{0} & \frac{\bar{\mathbf{A}}_f-\bar{\mathbf{B}}_f\mathbf{K}_f}{\mu}\end{bmatrix}\begin{bmatrix}\mathbf{x}_s\\ \mathbf{x}_f\end{bmatrix} \tag{60}$$

so as to place $\lambda((\bar{\mathbf{A}}_f - \bar{\mathbf{B}}_f\mathbf{K}_f)/\mu)$ at desired locations. Therefore, the overall input for the system (35), consequently for system (32), can be obtained from (52), (54), (56), and (59) as

$$\mathbf{u} = -\hat{\mathbf{K}}\begin{bmatrix}\mathbf{x}_a^T & \mathbf{x}_b^T\end{bmatrix}^T = -\hat{\mathbf{K}}\mathbf{x} \tag{61}$$

where

$$\hat{\mathbf{K}} = \begin{bmatrix}\mathbf{K}_s - \mathbf{K}_f\mathbf{M} & \mu(\mathbf{K}_s - \mathbf{K}_f\mathbf{M})\mathbf{P} + \mathbf{K}_f\end{bmatrix}. \tag{62}$$

This is the composite feedback gain, derived from subsystem feedback gains designed independently, so that the original system (16) is asymptotically stable, i.e., $\lambda(\hat{\mathbf{A}} - \hat{\mathbf{B}}\hat{\mathbf{K}}) < 0$.

Remark 1: It is interesting to note the following points.

1) Compared to three equations in [24], only two nonsymmetric Riccati equations (38) and (42), respectively, for $\mathbf{P}$ and $\mathbf{P}_s$ are needed to solve to get lower triangular form (44) of (32). Again, in contrast to three equations in [24], the solutions of simply two Sylvester equations (49) and (58), respectively, for $\mathbf{M}_s$ and $\mathbf{M}$ are required to perform the three-stage design. The solutions of these algebraic equations can be obtained using the fixed-point iteration method used in [24].
2) Although only four algebraic equations are required to be solved in comparison to six equations in [24], these four equations are of higher order than six equations in [24]. Hence, floating point operations (FLOPs) required to find the solution, expressed as a function of the matrix dimension, are determined and compared for both the methods. If n_1, n_2, and n_3 are the orders of the slow, fast, and very fast subsystems, inequality

$$2n^3 + 6h^3 + \frac{2}{3}n_3^3 + n^2 + n_3^2 > 2h^2(1+4n) + 4n_1n_2n_3 \tag{63}$$

is derived, in which $n = n_1 + n_2 + n_3$ and $h = n_1 + n_2$. It is noticed that the online computational requirements will be reduced by the proposed method if the inequality (63) is satisfied.
3) In addition, the offline computational requirements are significantly reduced as calculations are done with the (2×2) matrix representation instead of (3×3) matrix representation, without the loss of accuracy and the

freedom to design different local feedback controllers for individual subsystems.

Remark 2: If $\lambda(\bar{\mathbf{A}}_f/\mu) < 0$, only "slow" and "fast" subsystems are needed to be stabilized by corresponding controls (45) and (50). Accordingly, $\mathbf{K}_f$ can be set to zero in (62), resulting in $\bar{\mathbf{K}} = [\mathbf{K}_s \ \mu\mathbf{K}_s\mathbf{P}]$, where $\mathbf{K}_s$ is given by (53).

Remark 3: In the presence of $\lambda\left(\frac{\bar{\mathbf{A}}_{sf}}{\epsilon}\right) < 0$ and $\lambda(\bar{\mathbf{A}}_f/\mu) < 0$, "slow" subsystem alone demands stabilization as per control (45). As a deduction, both $\mathbf{K}_{sf}$ and $\mathbf{K}_f$ can be replaced with zeros in (53) and (62), respectively, ending with gain as $\tilde{\mathbf{K}} = [\tilde{\mathbf{K}}_s \ \mu\tilde{\mathbf{K}}_s\mathbf{P}]$, where $\tilde{\mathbf{K}}_s = [\mathbf{K}_{ss} \ \epsilon\mathbf{K}_{ss}\mathbf{P}_s]$.

In case of controller formulation as per Remark 2, one has to deal with three algebraic equations, i.e., for $\mathbf{P}$, $\mathbf{P}_s$, and $\mathbf{M}_s$, while, in controller design, using Remark 3 only two equation, namely, for $\mathbf{P}$ and $\mathbf{P}_s$. This further cuts down computations.

2) Design of Observer Gain ($\mathbf{L}$)*:* Designing an observer gain for (13)-(14) is analogous to solving an eigenvalue assignment problem for the dual system

$$\dot{\eta} = \mathbf{A}^T\eta + \mathbf{C}^T\nu \tag{64}$$

$$\xi = \mathbf{B}^T\nu \tag{65}$$

with control $\nu = \mathbf{L}^T\eta$, such that $\lambda(\mathbf{A} - \mathbf{LC}) < 0$, provided Assumption 1 is fulfilled. Note that dual system (64)-(65) also displays three-time-scale property, because $\lambda(\mathbf{A}) = \lambda(\mathbf{A}^T)$. And so, for the suggested three-stage observer design, consider an analogous system to (30)-(31) [21] as

$$\begin{bmatrix}\dot{\eta}_1\\ \dot{\eta}_2\\ \dot{\eta}_3\end{bmatrix} = \begin{bmatrix}\mathbf{A}_{o11}^T & \frac{\mathbf{A}_{o21}^T}{\epsilon} & \frac{\mathbf{A}_{o31}^T}{\mu}\\ \mathbf{A}_{o12}^T & \frac{\mathbf{A}_{o22}^T}{\epsilon} & \frac{\mathbf{A}_{o32}^T}{\mu}\\ \mathbf{A}_{o13}^T & \frac{\mathbf{A}_{o23}^T}{\epsilon} & \frac{\mathbf{A}_{o33}^T}{\mu}\end{bmatrix}\begin{bmatrix}\eta_1\\ \eta_2\\ \eta_3\end{bmatrix} + \begin{bmatrix}\mathbf{C}_{o1}^T\\ \mathbf{C}_{o2}^T\\ \mathbf{C}_{o3}^T\end{bmatrix}\nu. \tag{66}$$

Introducing

$$\begin{bmatrix}\mathbf{q}_1\\ \mathbf{q}_2\\ \mathbf{q}_3\end{bmatrix} = \begin{bmatrix}\mathbf{I}_{n1} & \mathbf{0} & \mathbf{0}\\ \mathbf{0} & \frac{\mathbf{I}_{n2}}{\epsilon} & \mathbf{0}\\ \mathbf{0} & \mathbf{0} & \frac{\mathbf{I}_{n3}}{\mu}\end{bmatrix}\begin{bmatrix}\eta_1\\ \eta_2\\ \eta_3\end{bmatrix} = \mathbf{T}\begin{bmatrix}\eta_1\\ \eta_2\\ \eta_3\end{bmatrix} \tag{67}$$

standard singularly perturbed three-time-scale form of (66) is obtained as

$$\begin{bmatrix}\dot{\mathbf{q}}_1\\ \dot{\mathbf{q}}_2\\ \dot{\mathbf{q}}_3\end{bmatrix} = \begin{bmatrix}\mathbf{A}_{o11}^T & \mathbf{A}_{o21}^T & \mathbf{A}_{o31}^T\\ \frac{\mathbf{A}_{o12}^T}{\epsilon} & \frac{\mathbf{A}_{o22}^T}{\epsilon} & \frac{\mathbf{A}_{o32}^T}{\epsilon}\\ \frac{\mathbf{A}_{o13}^T}{\mu} & \frac{\mathbf{A}_{o23}^T}{\mu} & \frac{\mathbf{A}_{o33}^T}{\mu}\end{bmatrix}\begin{bmatrix}\mathbf{q}_1\\ \mathbf{q}_2\\ \mathbf{q}_3\end{bmatrix} + \begin{bmatrix}\mathbf{C}_{o1}^T\\ \frac{\mathbf{C}_{o2}^T}{\epsilon}\\ \frac{\mathbf{C}_{o3}^T}{\mu}\end{bmatrix}\nu \tag{68}$$

where $\mathbf{q}_1 \in \Re^{n_1}$, $\mathbf{q}_2 \in \Re^{n_2}$, and $\mathbf{q}_3 \in \Re^{n_3}$. The three-stage design of an observer gain can be completed exactly in a similar manner as that of feedback gain, mentioned in Section III-B1 from (34) to (62), namely, constructing lower triangular form of (68) and exercising three stages of design for observer gain to get $\mathbf{L}_{ss}$, $\mathbf{L}_{sf}$, and $\mathbf{L}_f$ at the end of each stage, such as $\mathbf{K}_{ss}$, $\mathbf{K}_{sf}$, and $\mathbf{K}_f$, respectively. However, the difference is in dimensions of the state transformations, as the observer gain is designed for the original system (30)-(31) and feedback gain is designed for the augmented system (32)-(33). Besides the final composite observer gain should be represented in the original states by using (67). While designing subsystem observer gains, care must be taken to meet Assumptions 3–5.

IV. Control Design and Application to CFPP

This section deliberates control design aspects first and after that its application to 300-MW CFPP under representative transients.

A. Controller Design

The three-time-scale structure of the 300-MW CFPP is identified in Section II. It has two outputs and six states. Applying an integral control makes the order of the augmented system (16) as eight. Hence according to Lemma 1, the order of "slow" mode increases from 2 to 4 with eigenvalues as $(0, 0, -0.0026, -0.0071)$. No change is observed in the location of eigenvalues of "fast," "very fast" modes. Ratios ϵ and μ also remain unchanged. The next step is to obtain the overall state feedback gain using merely "slow" subsystem states, because of stable "fast" and "very fast" states. It is worth noting that the augmented model of CFPP is in implicit singularly perturbed form. Hence, it is transformed into explicitly singularly perturbed form by replacing some rows of the system matrix such that inverses of $\mathbf{A}_{22}$ and $\mathbf{A}_{33}$ exist [26]. After that, with suggested divisions and mergers of states, the system (38) is solved to get $\mathbf{P}$ which helps to find $\bar{\mathbf{A}}_f$ and $\bar{\mathbf{A}}_s$. Here, one can affirm that the eigenvalues of $\bar{\mathbf{A}}_f$ are one and the same as that of "very fast" mode, whereas eigenvalues of $\bar{\mathbf{A}}_s$ are the union of "slow" and "fast" modes. Now solving (42) provides $\mathbf{P}_s$. Resultantly, one can gain $\bar{\mathbf{A}}_{ss}$ and $\bar{\mathbf{A}}_{sf}$. Again, it is checked that the eigenvalues of $\bar{\mathbf{A}}_{ss}$ and $\bar{\mathbf{A}}_{sf}$ are equivalent to the eigenvalues of "slow" and "fast" modes, respectively. Considering no requirement of controls for "fast" and "very fast" modes, the desired eigenvalues of "slow" subsystem are selected as $(-0.97, -0.86, -0.75, -0.64) \times 10^{-3}$, and these are accurately placed by determining feedback gain $\mathbf{K}_{ss}$. Substituting $\mathbf{K}_{sf} = 0$, the feedback gain at the end of second stage is obtained and again making $\mathbf{K}_f = 0$, one can have $\tilde{\mathbf{K}}$, after third stage. The closed-loop eigenvalues, i.e., $\lambda(\hat{\mathbf{A}} - \hat{\mathbf{B}}\tilde{\mathbf{K}})$ are found to be precisely placed at

$$\lambda_{cl} = \big[-0.00064 \ -0.00075 \ -0.00086 \ -0.00097 \ -0.0454 \ -0.1306 \pm j0.0361 \ -0.2497\big]. \tag{69}$$

The maximum value of the feedback gain is -19.0392, which seems to be practically realizable. Feedback gain, by the direct design, to place the eigenvalues at locations (69) is also calculated. With the desire to implement controller, observer gains are determined for (13) using both three-stage design and direct design to place observer poles at $(-3.7455, -1.9590 \pm j0.5415, -0.0683, -0.0146, -0.0129)$. The gains obtained by the procedure of [24] are noticed to be the same. On the contrary, the FLOPs are observed to be more, as the inequality (63) is satisfied. FLOPs required for determining feedback and observer gains by the proposed method are 1092 and 528, respectively, whereas as per [24], respectively, 1259 and 711 FLOPs are required.

B. Simulation Results

Simulation results due to feedback gains obtained by the proposed three-stage design and direct design are generated and compared with DEB-based PI (DEB-PI) controller [10].

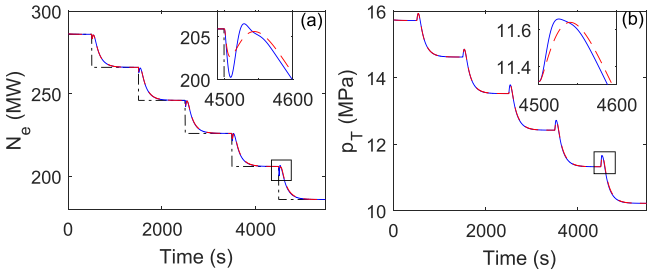

Fig. 1. Effect of change in operating conditions from 285.9 to 185.9 MW on (a) electrical power and (b) throttle pressure (black dashed-dotted line: set point; blue solid line: three-stage design; red dashed line: DEB-PI).

TABLE I
COMPARISON OF THREE-STAGE DESIGN AND DEB-PI

Operating Conditions (MW)		285.9-265.9	265.9-245.9	245.9-225.9	225.9-205.9	205.9-185.9
IAE	Three-Stage	118.27	118.48	118.68	118.90	119.13
	DEB-PI	118.85	120.24	121.79	123.51	125.48
ISE	Three-Stage	1487.9	1491.9	1496.0	1501.0	1508.3
	DEB-PI	1490.7	1511.5	1536.2	1566.6	1604.8

Before initiating any transient, it is ensured that the plant (1)–(8) is at steady state. To start with, estimation errors with both the observer gains (i.e., three-stage and direct design) are compared to evaluate their convergence. It is observed that the convergence with the three-stage design is better than the direct design. Hence, in all the cases, observer gain obtained with the three-stage design is used.

1) Tracking Performance: In this case, the operating condition, starting at 500 s, is slowly decreased from 285.9 MW by 20 MW after every 1000 s, as shown in Fig. 1(a). Corresponding variations in throttle pressure are shown in Fig. 1(b). It is learned that as the operating point decreases, response due to directly designed feedback control starts oscillating with an increasing amplitude and becomes unstable after 225.9 MW. Hence, it is not shown in Fig 1. However, with three-stage design and DEB-PI, the overall response was found to be stable with tracking rate of output power as 1.6% of the full load per minute [Fig, 1(a)]. In addition, the reverse response of the throttle pressure is also inspected to be within ± 0.4 MPa [refer inset of Fig. 1(b)]. As the proposed control and DEB-PI are showing identical responses, their results are compared by calculating error indices for power as tabulated in Table I. Table I displays the improvement in suggested three-stage design over DEB-PI.

2) Regulating Performance: First, boiler demand is cut by 5% of the nominal value after 50 s and then restored. Effect of this on the output power and throttle pressure is supervised in Fig. 2. Second, a throttle opening position is dropped by 5% after 50 s and regained later. Influence of this on the power and pressure is represented in Fig. 3. In both the cases, power and pressure are efficiently regulated by all the controllers. Collectively, the response due to proposed three-stage design is observed to be superior to other two controllers.

3) Disturbance Rejection and Robustness: Here, the effect of coal quality variation is studied with 20% quick increase at 100 s and then continuous variation with the period of 628 s after 2100 s. For the abrupt change, both power and pressure are controlled by all the controllers as reflected in Fig. 4.

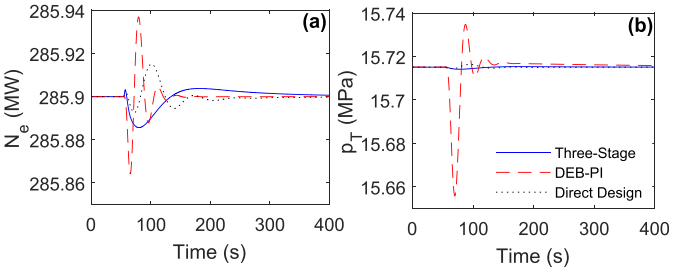

Fig. 2. Effect of 5% variation in boiler demand on (a) electrical power and (b) throttle pressure.

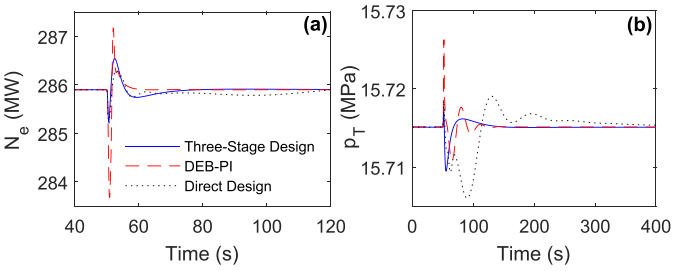

Fig. 3. Effect of 5% variation in throttle opening position on (a) electrical power and (b) throttle pressure.

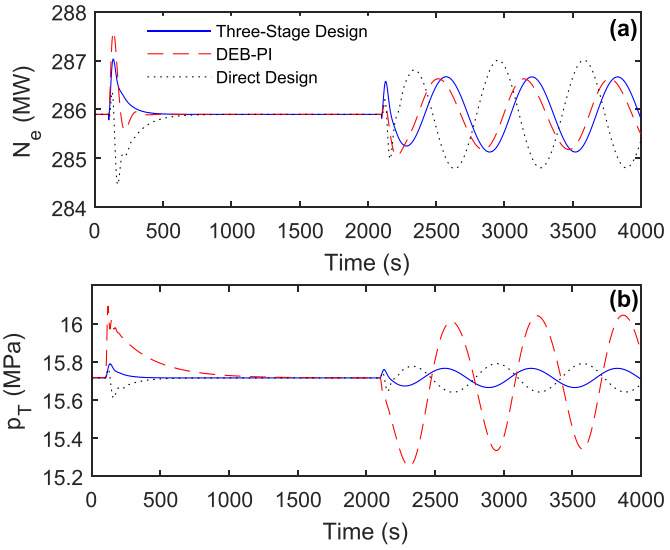

Fig. 4. Effect of change in coal quality on (a) electrical power and (b) throttle pressure.

However, response due to three-stage design is found to be better than direct design and DEB-PI. For periodic fluctuations, power shows oscillations of nearly the same magnitude and pressure shows oscillations of lesser magnitude as that obtained with DEB-PI. Corresponding variations in control inputs, displayed in Fig. 5, also indicate the performance improvement by three-stage design over the direct design and DEB-PI. Although the sudden change in coal quality is handled competently, periodic changes result in oscillations in power and pressure. This is due to the strong couplings between the main steam pressure control loop and the power output control loop. Finally, to assess the robustness of controllers for parameter uncertainty, the set-point variations with the change in the dynamic constants given in [10] are observed. Here, the control due to direct design resulted in an

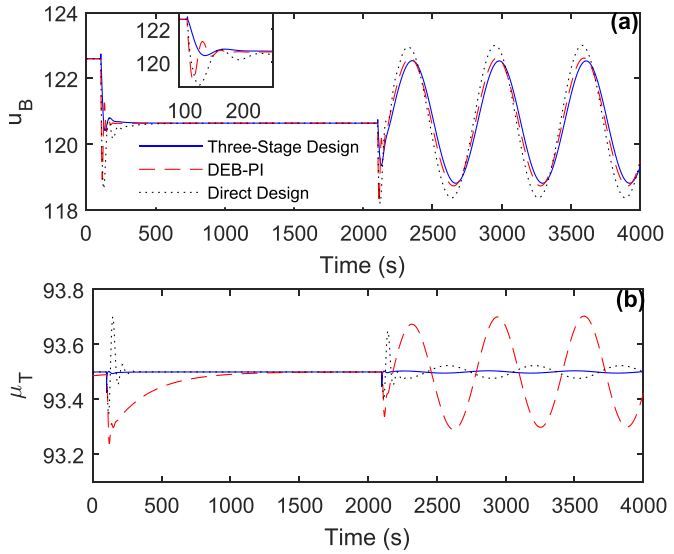

Fig. 5. Effect of change in coal quality on control inputs. (a) Boiler demand (t/h). (b) Throttle opening position (%).

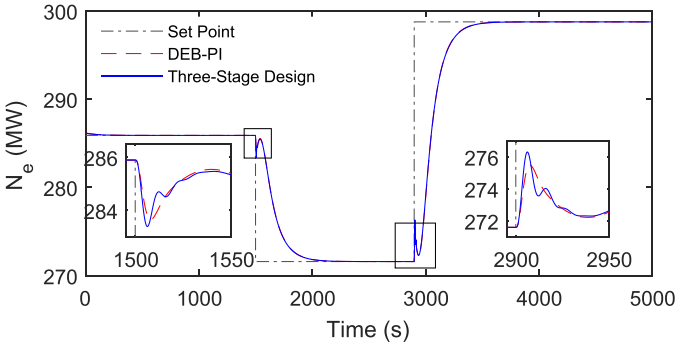

Fig. 6. Effect of parameter uncertainty on electrical power.

unstable response, whereas the three-stage design and DEB-PI gave responses as illustrated in Fig. 6. The instants of set-point initiations are shown in the inset of Fig. 6.

V. Conclusion

In this brief, an observer-based output feedback control using an integral action for a three-time-scale system is proposed in which both feedback and observer gains are designed in three stages using the two-time-scale approach. The presented three-stage design method offers significant online and offline computation savings and obviates ill-conditioning concerns of the higher order multitime-scale system. The effectiveness and merits of the proposed controller are validated through the nonlinear simulations of a large-scale 300-MW CFPP. From simulations, it is observed that the suggested controller achieves significant tracking and regulating control in the presence of input and parameter perturbations compared to direct design approach and DEB-based PI controller and meets the stringent control requirements of the practical power plant. The controller design with the input time delay compensation may be considered in the future.

References

[1] *Annual Energy Outlook 2017 With Projections to 2050*, U.S. Energy Inf. Admin., Washington, DC, USA, Jan. 2017.

[2] *Key World Energy Statistics 2017*, Int. Energy Agency, Paris, France, 2017.

[3] S. Chandrasekharan, R. C. Panda, and B. N. Swaminathan, "Modeling, identification, and control of coal-fired thermal power plants," *Rev. Chem. Eng.*, vol. 30, no. 2, pp. 217–232, 2014.

[4] X. Wu, J. Shen, Y. Li, and K. Y. Lee, "Steam power plant configuration, design, and control," *Wiley Interdiscipl. Rev., Energy Environ.*, vol. 4, no. 6, pp. 537–563, 2015.

[5] H. Peng, T. Ozaki, V. Haggan-Ozaki, and Y. Toyoda, "A nonlinear exponential ARX model-based multivariable generalized predictive control strategy for thermal power plants," *IEEE Trans. Control Syst. Technol.*, vol. 10, no. 2, pp. 256–262, Mar. 2002.

[6] S. Li, H. Lui, W.-J. Cai, Y.-C. Soh, and L.-H. Xie, "A new coordinated control strategy for boiler-turbine system of coal-fired power plant," *IEEE Trans. Control Syst. Technol.*, vol. 13, no. 6, pp. 943–954, Nov. 2005.

[7] X. Liu, P. Guan, and C. W. Chan, "Nonlinear multivariable power plant coordinate control by constrained predictive scheme," *IEEE Trans. Control Syst. Technol.*, vol. 18, no. 5, pp. 1116–1125, Sep. 2010.

[8] N. Alamoodi and P. Daoutidis, "Nonlinear decoupling control with deadtime compensation for multirange operation of steam power plants," *IEEE Trans. Control Syst. Technol.*, vol. 24, no. 1, pp. 341–348, Jan. 2016.

[9] N. Alamoodi and P. Daoutidis, "Nonlinear control of coal-fired steam power plants," *Control Eng. Pract.*, vol. 60, pp. 63–75, Mar. 2017.

[10] L. Sun, D. Li, K. Y. Lee, and Y. Xue, "Control-oriented modeling and analysis of direct energy balance in coal-fired boiler-turbine unit," *Control Eng. Pract.*, vol. 55, pp. 38–55, Oct. 2016.

[11] L. Sun, Q. Hua, D. Li, L. Pan, Y. Xue, and K. Y. Lee, "Direct energy balance based active disturbance rejection control for coal-fired power plant," *ISA Trans.*, vol. 70, pp. 486–493, Sep. 2017.

[12] H. Moradi and G. Vossoughi, "Multivariable optimal control of an industrial nonlinear boilerâŁ"turbine unit," *Meccanica*, vol. 51, pp. 859–875, Apr. 2016.

[13] M. Gamal, M. El-Banna, and M. M. Farag, "Hardware implementation of an LQR controller of a drum-type boiler turbine on FPGA," in *Proc. 28th IEEE Int. Conf. Microelectron.*, Dec. 2016, pp. 137–140.

[14] L. Wei and F. Fang, "H_∞-LQR-based coordinated control for large coal-fired boiler–turbine generation units," *IEEE Trans. Ind. Electron.*, vol. 64, no. 6, pp. 5212–5221, Jun. 2017.

[15] Y. Zhang, D. S. Naidu, C. Cai, and Y. Zou, "Singular perturbations and time scales in control theories and applications: An overview 2002–2012," *Int. J. Inf. Syst. Sci.*, vol. 9, no. 1, pp. 1–36, 2014.

[16] D. S. Naidu and A. K. Rao, "Application of the singular perturbation method to a steam power system," *Electr. Power Syst. Res.*, vol. 8, no. 3, pp. 219–226, 1985.

[17] B. M. Patre, B. Bandyopadhyay, and H. Werner, "Periodic output feedback control for singularly perturbed discrete model of steam power system," *IEE Proc. Control Theory Appl.*, vol. 146, no. 3, pp. 247–252, May 1999.

[18] R. Cori and C. Maffezzoni, "Practical-optimal control of a drum boiler power plant," *Automatica*, vol. 20, no. 2, pp. 163–173, 1984.

[19] R. Phillips, "A two-stage design of linear feedback controls," *IEEE Trans. Autom. Control*, vol. AC-25, no. 6, pp. 1220–1223, Dec. 1980.

[20] V. Radisavljevic-Gajic and P. Rose, "A new two-stage design of feedback controllers for a hydrogen gas reformer," *Int. J. Hydrogen Energy*, vol. 39, no. 22, pp. 11738–11748, 2014.

[21] H. Yoo and Z. Gajic, "New designs of linear observers and observer-based controllers for singularly perturbed linear systems," *IEEE Trans. Autom. Control*, vol. 63, no. 11, pp. 3904–3911, Nov. 2018.

[22] D. S. Naidu and R. Ravinder, "On three time scale analysis," in *Proc. IEEE Conf. Decis. Control*, Dec. 1985, pp. 81–85.

[23] N. P. Singh, Y. P. Singh, and S. I. Ahson, "An iterative approach to reduced-order modeling of synchronous machines using singular perturbation," *Proc. IEEE*, vol. 74, no. 6, pp. 892–893, Jun. 1986.

[24] V. Radisavljevic-Gajic, M. Milanovic, and G. Clayton, "Three-stage feedback controller design with applications to three time-scale linear control systems," *ASME J. Dyn. Syst., Meas., Control*, vol. 139, pp. 1–10, Oct. 2017.

[25] C.-T. Chen, *Linear System Theory and Design*. New York, NY, USA: Oxford Univ. Press, 1999.

[26] D. S. Naidu, *Singular Perturbation Methodology in Control Systems*. London, U.K.: Peter Peregrinus, 1988.